PCCP

Microelectrochemical measurements of electron transfer rates at the interface between two immiscible electrolyte solutions: Potential dependence of the ferro/ferricyanide-7,7,8,8-tetracyanoquinodimethane (TCNQ)/TCNQ$^{\bullet -}$ system

Jie Zhang and Patrick R. Unwin*

Department of Chemistry, University of Warwick, Coventry, UK CV4 7AL.
E-mail: P.R.Unwin@warwick.ac.uk

Received 1st October 2001, Accepted 9th April 2002
First published as an Advance Article on the web 4th July 2002

The reduction of 7,7,8,8-tetracyanoquinodimethane (TCNQ) in both 1,2-dichloroethane (DCE) and nitrobenzene (NB), by aqueous ferrocyanide, and the back reaction have been studied by scanning electrochemical microscopy (SECM) and microelectrochemical measurements at expanding droplets (MEMED). The main focus has been to elucidate the effect of galvanic potential at the interface between two immiscible electrolyte solutions (ITIES) on electron transfer (ET) rates, with different electrolyte concentrations in the organic phase. SECM studies show that the ET rate constants for both the forward and back reaction depend strongly on the interfacial potential drop, with an apparent ET coefficient close to 0.5. MEMED demonstrates that TCNQ$^{\bullet -}$ is confined to DCE, but transfers from NB to water under certain experimental conditions, which could complicate kinetic analysis. The ET kinetics for the water/DCE system have been analysed further using Marcus theory. Close to zero driving force, the rate constants for the forward and back reaction are found to be similar and in good agreement with predictions from Marcus theory with a sharp liquid/liquid interface. The results suggest that Butler–Volmer kinetics describe ET at the ITIES when the driving force is low and the ionic strength in both the aqueous and organic phases is relatively high.

Introduction

Understanding the potential-dependence of rates of electron transfer (ET) across the interface between two immiscible electrolyte solutions (ITIES) is currently an area of considerable research activity. Several techniques have recently been applied to a number of redox systems, but with quite different results and conclusions.[1–16]

In previous scanning electrochemical microscopy (SECM) measurements of the reaction rate between cationic 5,10,15,20-tetraphenyl-21H,23H-porphine zinc ($ZnPor^+$) in benzene or benzonitrile and various aqueous reductants,[1,2] a Butler–Volmer trend was observed at low driving force,[1] together with behaviour consistent with Marcus theory over a wide range of driving force.[1b,2,3] The reduction of the neutral species, 7,7,8,8-tetracyanoquinodimethane (TCNQ), in 1,2-dichloroethane (DCE) by electrogenerated $Fe(CN)_6^{4-}$ has been studied extensively with both SECM and microelectrochemical measurements at expanding droplets (MEMED).[4] The measured ET rates showed a strong dependence on the interfacial potential drop with an ET coefficient (α) in the range 0.4–0.7, with a relatively high ionic strength in both the water and DCE phases. The kinetics of the reverse reaction were also reported recently in a preliminary communication;[5] Butler–Volmer behaviour was observed, with a bimolecular rate constant of 0.06 cm s^{-1} M^{-1} at zero driving force. Similar characteristics for this redox system were also reported independently by Ding *et al.*[3] and Shi and Anson.[6] However, an earlier spectroelectrochemical study suggested that the potential-dependence of the reduction of TCNQ by aqueous ferrocyanide did not show a pure Butler–Volmer trend.[7]

The potential dependence of ET processes at the ITIES has also been established by conventional four-electrode voltammetric studies[8,9] and photocurrent measurements.[7,10,11,12] In the latter case, Girault and co-workers recently studied the heterogeneous quenching of water-soluble zinc tetrakis(carboxyphenyl) porphyrin (ZnTPPC) by ferrocene and diferrocenylethane in DCE. An α value of 0.32 was measured in the region close to the potential of zero charge.[10] The same group also studied the photoinduced ET process between aqueous ZnTPPC and a wide range of organic quenchers. It was found that the Gibbs energy of activation for the charge transfer process was affected by the galvanic potential difference.[11] For photoinduced ET between aqueous neutral ion-pairs and the neutral electron donors decamethylferrocene (DMFc) and TCNQ in DCE, an α value of 0.5 was estimated.[12]

There have been several recent reports of the potential-independence of ET rates at ITIES.[13,16] The observations derived from a thin layer method were attributed to the formation of precursor complexes within the interfacial region, as the rate-determining step, which would be little influenced by the driving force for the subsequent, faster, ET step.[13] Some of the systems studied showed behaviour contrary to Butler–Volmer kinetics,[13] as supported by SECM data.[14] However, a number of results from the thin layer method may also be complicated by uncompensated diffusional limitations.[6,15]

Liu and Mirkin[16] studied the ET reaction between aqueous redox species (*e.g.* $Ru(CN)_6^{3-}$) and neutral organic species (*e.g.* ZnPor) using SECM, with the potential drop across the ITIES established with ClO_4^- salts in each phase. The measured ET rate constants were found to be independent of the interfacial potential drop, but dependent on the driving force

 DOI: 10.1039/b108882c

contributed by the aqueous redox species. It was concluded that this result agreed with Schmickler's recent model for ET at the ITIES.[17] It was further suggested that the α value obtained in previous studies[1a] may have been compromised by interfacial concentration effects.[17,18]

Following our previous study on the one-electron reduction of TCNQ to $TCNQ^{\bullet-}$ by aqueous $Fe(CN)_6^{4-}$,[4,5] we further investigate this reaction and the back reaction (oxidation of $TCNQ^{\bullet-}$ by ferricyanide) over a much wider range of conditions. In addition to DCE, used as the organic solvent previously, we also investigate the ET reaction with nitrobenzene (NB) as the organic solvent. The processes of interest can be represented as,

$$TCNQ + Fe(CN)_6^{4-} \underset{k_b}{\overset{k_f}{\rightleftharpoons}} TCNQ^{\cdot-} + Fe(CN)_6^{3-} \quad (1)$$

where k_f and k_b are the effective bimolecular rate constants for the oxidation of $Fe(CN)_6^{4-}$ (reduction of TCNQ) and reduction of $Fe(CN)_6^{3-}$ (oxidation of $TCNQ^{\bullet-}$), respectively.

TCNQ was selected for study because it has been widely used for investigations of ET at ITIES, particularly with techniques employing externally polarised ITIES.[7,8,19] Moreover, as highlighted above, recent studies[3–6] confirm that TCNQ/$Fe(CN)_6^{4-}$ is a suitable system for investigating the factors affecting ET reactions at ITIES. The potential drop across the ITIES was varied by using ClO_4^- as a common potential determining ion in the two phases. A specific interest in this paper was to determine k_f and k_b close to zero driving force, and to carefully investigate the possibility of facilitated ion transfer processes which may complicate the measured ET kinetics and potential-dependent behaviour.

Experimental section

Chemicals

Potassium hexacyanoferrate (A.R.), NaCl (A.R.) (both from Fisons), sodium hexacyanoferrate(II) decahydrate (Strem), TCNQ (98%, Lancaster), tetra-n-hexylammonium perchlorate (THAP, crystalline, Alfa), $NaClO_4 \cdot xH_2O$ (A.R.), NB (99+%) and DCE (HPLC grade) (all from Sigma-Aldrich) were used as received. All aqueous solutions were prepared from Milli-Q reagent water (Millipore Corp.).

Apparatus and procedures

Electrochemical measurements were made under controlled ambient conditions ($23 \pm 0.5\,^{\circ}C$) using a two-electrode arrangement. Either a saturated calomel electrode (SCE) or silver quasi-reference electrode (AgQRE) served as the reference electrode, and a glass-coated Pt ultramicroelectrode (UME, either 2 or 25 μm diameter) functioned as the working electrode tip. The UME had a defined *RG* value of 10 for SECM measurements which employed a 25 μm diameter tip, and 4 for MEMED measurements which utilised the 2 μm diameter probe. $RG = r_s/a$, where r_s is the overall radius of the tip end (electrode plus insulating sheath) and a is the electrode radius. The electrodes were fabricated and polished as described previously.[20]

To measure the heterogeneous rate constants for the reaction between $Fe(CN)_6^{4-}$ and TCNQ using SECM, a flat interface was established in a conventional cell,[20,21] between an aqueous (top) phase and an organic (bottom) phase. The aqueous phase contained 1 mM $Fe(CN)_6^{3-}$, 0.1 M NaCl and 0.01–0.25 M $NaClO_4$, while the organic phase contained 10 mM TCNQ and either 0.1 M or 0.01 M THAP. The tip, in the aqueous phase, was used to reduce $Fe(CN)_6^{3-}$ to $Fe(CN)_6^{4-}$ at a diffusion-controlled rate.

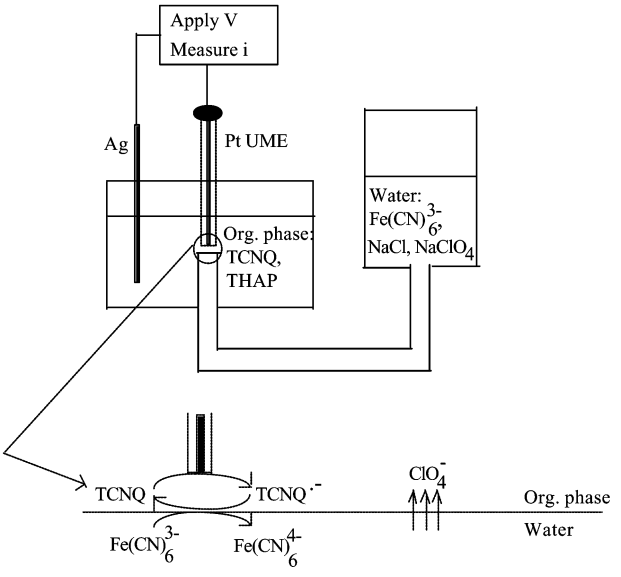

Fig. 1 Schematic of the application of SECM in the measurement of ET reactions at the aqueous/organic interface when the organic solution forms the top phase.

The heterogeneous rate constants for the reverse reaction between $Fe(CN)_6^{3-}$ and $TCNQ^{\bullet-}$ were measured by SECM, using a method similar to that proposed by Mirkin and coworkers.[22] The aqueous phase was held at the tip of a glass tube positioned through the base of the cell (Fig. 1). The bottom aqueous phase contained either 10 or 20 mM $Fe(CN)_6^{3-}$, 0.1 M NaCl and 0.01–1.0 M $NaClO_4$, while the organic phase (top) contained 1 mM TCNQ, and either 0.1 or 0.01 M THAP. In this configuration, the tip UME was positioned in the organic phase and used to locally generate $TCNQ^{\bullet-}$ by the diffusion-limited reduction of TCNQ.

The basic apparatus used for SECM has been described previously.[4,5,20,21] Approach curves were obtained by translating the tip towards the ITIES and recording the steady-state current as a function of d (the distance between the tip and the ITIES). When the tip attained the distance closest approach to the ITIES, there was either a plateau in current–distance characteristics (for the case of the UME in the aqueous phase) or sudden change in current (for the case of the UME in the organic phase). Typically, a 25 μm diameter tip could be approached to a distance of *ca.* 1–2 μm from the ITIES (UME in the aqueous phase) or 2–3 μm (UME in the organic phase). To determine this distance precisely, negative feedback experiments were always run without any redox-active species in the bottom phase and data analysed with negative feedback theory similar to that of Kwak and Bard.[23]

In MEMED, concentration profiles of both reactant and product were determined. To measure the concentration profile of aqueous $Fe(CN)_6^{4-}$, an organic drop containing 10 mM TCNQ and 0.01 M THAP was grown into an aqueous receptor phase containing 1 mM $Fe(CN)_6^{4-}$, 0.1 M NaCl and 0.01–0.25 M $NaClO_4$, from a capillary with an internal diameter of about 200 μm. The concentration profiles of TCNQ and $TCNQ^{\bullet-}$ in the organic receptor phase, were measured by growing water droplets containing 50 mM $Fe(CN)_6^{4-}$, 0.1 M NaCl and 0.01–0.25 M $NaClO_4$, into the organic phase containing 1 mM TCNQ and 0.01 M THAP. Amperometeric detection was used, which involved recording the current for the species of interest in the receptor phase, as the drop grew towards the tip.

In contrast to SECM, the small size of the tip used for MEMED meant that the electrode was a non-invasive probe

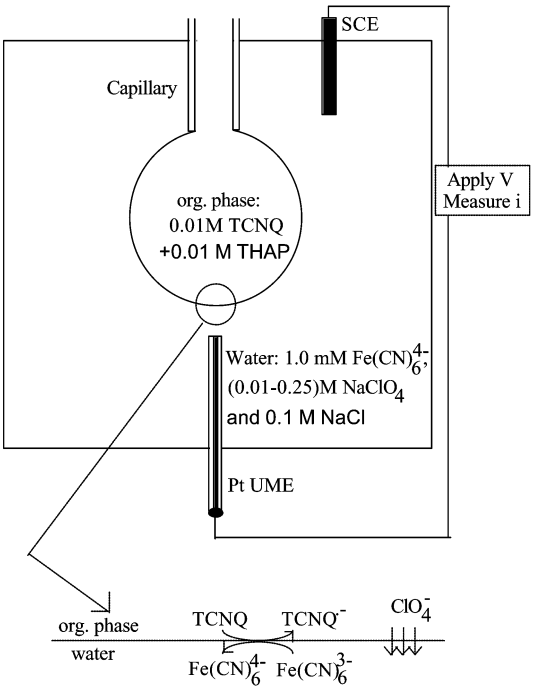

Fig. 2 Schematic of MEMED.

of the concentration boundary layer that developed adjacent to expanding droplets.[24] Fig. 2 shows a schematic of MEMED for the situation where organic droplets were grown into the aqueous receptor phase. For this particular case, the droplets were formed from a capillary placed above the electrode, because DCE is more dense than water. An inverted arrangement was used when aqueous droplets were grown into an organic receptor phase. A method for obtaining the time-dependent droplet concentration profile, from the UME response, has been outlined fully elsewhere.[25]

ClO_4^- was the only ion common to both phases in all of the experiments. The electroneutrality of the two phases was maintained by the transfer of this common ion when the ET reaction occurred at the ITIES. The ratio of the bulk activities of ClO_4^- in the aqueous and organic phases, determined the interfacial potential drop. At standard temperature and pressure, and assuming appropriate experimental conditions where the activity coefficients of ClO_4^- in the aqueous and DCE phases are maintained constant, within the concentration range of interest, the following equation should hold:[1–5]

$$\Delta_w^o\phi = \Delta_w^o\phi^{o'} - 0.059\ \log_{10}\frac{[ClO_4^-]_w}{[ClO_4^-]_o} \quad (2)$$

where $\Delta_w^o\ \phi = \phi_o - \phi_w$ is the Galvani potential (V) established across the interface; ϕ_o is the potential of the organic phase and ϕ_w is the aqueous phase potential. The formal transfer potential for ClO_4^- is given by

$$\Delta_w^o\phi^{o'} = \Delta_w^o\phi^o - 0.059\ \log_{10}\frac{\gamma_w}{\gamma_o} \quad (3)$$

where $\Delta_w^o\phi^o$ is standard transfer potential for ClO_4^-, γ_w and γ_o are the activity coefficients of ClO_4^- in water and the organic phase, respectively.

Diffusion coefficients of 1.05×10^{-5} cm^2 s^{-1} and 1.2×10^{-5} cm^2 s^{-1} (in DCE), and 4.8×10^{-6} cm^2 s^{-1} and 5.5×10^{-6} cm^2 s^{-1} (in NB) for TCNQ and TCNQ$^{\bullet-}$, respectively, were measured using both double potential step chronoamperometry[14,21b,c] and steady-state linear sweep voltammetry.[1,4]

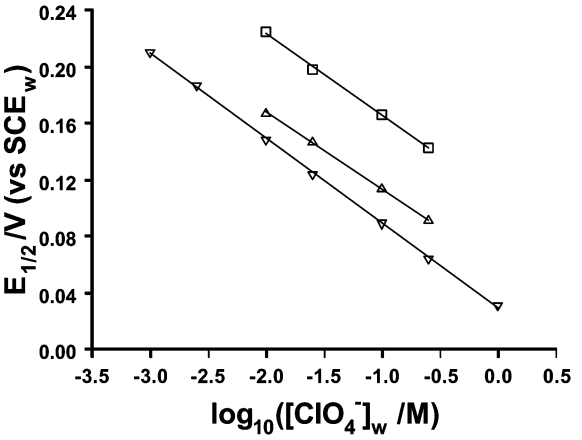

Fig. 3 Dependence of the half-wave potential for the reversible first reduction of TCNQ in either DCE or NB on $[ClO_4^-]_w$, with 0.01 M THAP in the DCE phase (▽), and either 0.1 M THAP (□) or 0.01 M THAP (△) in the NB phase.

Results and discussion

Potential drop across the ITIES

The relative values of the potential drop across the liquid/liquid interface were obtained by adopting the procedure advocated by Bard and co-workers.[1a] Steady-state linear sweep voltammograms for the first reduction of TCNQ at a 25 μm diameter microdisc electrode in each of the organic phases, were measured with respect to an SCE positioned in a contacting aqueous phase. The reversible half-wave potential ($E_{1/2}$) was derived from the voltammograms.

The dependence of $E_{1/2}$ on $[ClO_4^-]_w$, deduced from these measurements, with $[THAP]_o$ fixed at defined values, is shown in Fig. 3. The slopes (*ca.* 59 mV per decade) of the straight lines agree well with the predictions of eqn. (2). Moreover, the potential shifts by *ca.* 60 mV when $[THAP]_o$ in the NB phase changes by an order of magnitude from 0.01 M to 0.1 M, again consistent with eqn. (2). Although the ionic strength of the aqueous phase changes in these measurements, the activity coefficients of the various aqueous ions are fairly insensitive to the ionic strength for these experiments and those that follow.[4]

Potential-dependence of ET rates for the forward and back reactions: SECM measurements

Previous SECM studies have suggested Butler–Volmer characteristics for the ITIES at low driving force.[1–5] In this case, k_f and k_b can be written in terms of the driving force for the reaction, χ,

$$k_f = k_o \exp\left(\frac{\alpha nF\chi}{RT}\right) \quad (4)$$

$$k_b = k_o \exp\left(\frac{-\beta nF\chi}{RT}\right) \quad (5)$$

where k_o is the standard rate constant at zero driving force, α and β are the ET coefficients for the forward and reverse reactions, respectively, F is Faraday's constant, n is the number of electrons transferred per redox event, R is the gas constant and T is temperature. The driving force is defined in terms of the forward reaction by:

$$\chi = \Delta E^{o'} + \Delta_w^o\phi \quad (6)$$

where $\Delta E^{o'} = E^{o'}_{TCNQ^{o'\bullet-}} - E^{o'}_{Fe(CN)_6^{3-/4-}}$, is the difference in the formal potentials of the redox couples in the organic and

aqueous phases, *versus* a common reference electrode in one phase.[26,27]

To accurately determine the driving force, the difference in the formal potentials of $TCNQ^{o/\bullet -}$ and $Fe(CN)_6^{3-/4-}$ was measured with respect to SCE in the aqueous phase.[1] Because the diffusion coefficients of TCNQ and $TCNQ^{-\bullet}$ are similar, as defined earlier, the measured reversible half-wave potential of TCNQ reduction was used as $E^{o\prime}$.[28] Since the measured $E_{1/2}$ for the ferro–ferricyanide couple may depend on the solution and electrode conditions,[29] the formal potential was obtained from measurements of the equilibrium, open-circuit potential over the range of conditions used in the kinetic studies.

The analysis that follows considers eqns. (4) and (5) in the following form:

$$\log_{10} k_f = \log_{10} k_o + \frac{\alpha n F \chi}{\ln(10) RT} \quad (7)$$

$$\log_{10} k_b = \log_{10} k_o - \frac{\beta n F \chi}{\ln(10) RT} \quad (8)$$

Investigations of the potential-dependence of ET rate constants, for the reaction between TCNQ and $Fe(CN)_6^{4-}$ and the back reaction between $TCNQ^{\bullet -}$ and $Fe(CN)_6^{3-}$ are developments of recent preliminary work.[5] Typical new results are shown in Figs. 4–6. In each case, the driving force was varied by changing the concentration of ClO_4^- in the aqueous phase, with fixed $[THAP]_o$. SECM approach curves have been fitted to the optimal rate constant using a numerical model described in full previously.[2]

The results in Figs. 4–6 demonstrate that the ET rate constant depends strongly on the interfacial potential drop across the ITIES. With 0.01 M THAP in DCE, an α value of 0.44 ± 0.03 and a β value of 0.53 ± 0.01 were obtained (Fig. 4). For comparison in a recent communication,[5] we obtained $\alpha = 0.56 \pm 0.04$ and $\beta = 0.58 \pm 0.02$ for the aqueous/DCE system with 0.1 M THAP in DCE. When NB was used as the organic solvent, an α value of 0.54 ± 0.04 and a β value of 0.50 ± 0.05 were obtained in the presence of 0.1 M THAP (Fig. 5) and a β value of 0.53 ± 0.03 was obtained for the reverse reaction in the presence of 0.01 M THAP (Fig. 6). The rate of the forward reaction under these latter conditions was rather low and the reaction could barely be observed by SECM.

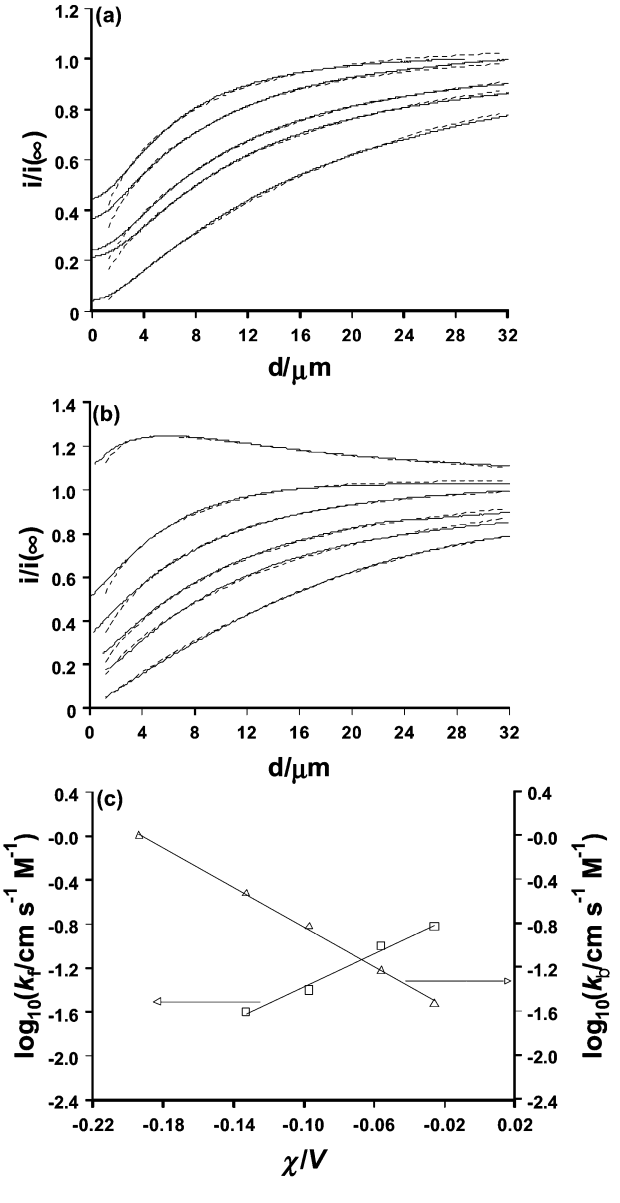

Fig. 4 Dependence of ET rate constants on driving force for the aqueous/DCE system. (a) SECM approach curves (ferricyanide reduction) for the forward reaction with 10 mM TCNQ and 0.01 M THAP in the DCE phase. From top to bottom, the first four solid experimental curves are for the following aqueous conditions: $[ClO_4^-]_w = 0.01$, 0.025, 0.1 and 0.25 M (1 mM $Fe(CN)_6^{3-}$ and 0.1 M NaCl). The corresponding dashed theoretical curves,[2] top to bottom, are for $k_f = 0.15$, 0.1, 0.04 and 0.025 cm s^{-1} M^{-1}. The lowest solid experimental curve was obtained in the absence of TCNQ in the DCE phase and the corresponding dashed curve is the theory for negative feedback.[23] (b) SECM approach curves (TCNQ reduction) for the reverse reaction with 1 mM TCNQ and 0.01 M THAP in the DCE phase. From top to bottom, the first five solid experimental curves are for $[ClO_4^-]_w = 1.0$, 0.25, 0.1, 0.025 and 0.01 M (10 mM $Fe(CN)_6^{3-}$ and 0.1 M NaCl) in the aqueous phase. The corresponding dashed theoretical curves, top to bottom, are for $k_b = 1.0$, 0.3, 0.15, 0.06 and 0.03 cm s^{-1} M^{-1}. The lowest solid experimental curve was obtained in the absence of $Fe(CN)_6^{3-}$ in the aqueous phase and the corresponding dashed curve is the theory for negative feedback. (c) Tafel plot of data in (a, □) and (b, △), constructed using eqns. (7) and (8).

Potential-dependence of ET rates for the forward reaction and observation of facilitated ion transfer using MEMED

To confirm the measured ET kinetics and determine whether there were any complications from facilitated ion transfer, MEMED was used to determine the rate constants for the forward reaction. Concentration profiles of $Fe(CN)_6^{4-}$ in the aqueous receptor phase, together with those for TCNQ and $TCNQ^{\bullet -}$ in the organic receptor phase were recorded according to the procedures described above. Typical results for the aqueous/DCE and aqueous/NB systems are shown in Figs. 7 and 8.

The results in Fig. 7 clearly indicate that the same bimolecular rate constants were measured for the water/DCE system whichever of the three species was detected. This illustrates that there are no complications from coupled $TCNQ^{\bullet -}$ transfer from DCE to water in the potential range of interest. Moreover, the measured rate constants derived from MEMED studies are comparable to those from SECM (Fig. 4). In contrast, while the concentration profile of TCNQ for the aqueous/NB system matches well to an ET rate constant, $k_f = 0.04$ cm s^{-1} M^{-1} (Fig. 8(a)), the corresponding $TCNQ^{\bullet -}$ concentrations are significantly lower than expected, based on the TCNQ profile. This suggests that $TCNQ^{\bullet -}$ is lost, possibly by transfer across the interface. This is confirmed by the clear deviation between the experimental profile of $Fe(CN)_6^{4-}$ (Fig. 8(b)) and that predicted based on the rate constant obtained from the TCNQ profile (Fig. 8(a)). The peak-shaped concentration profile, which is higher than the theoretical simulation, suggests that an additional electroactive species diffuses from the surface of the droplet into the aqueous phase, as

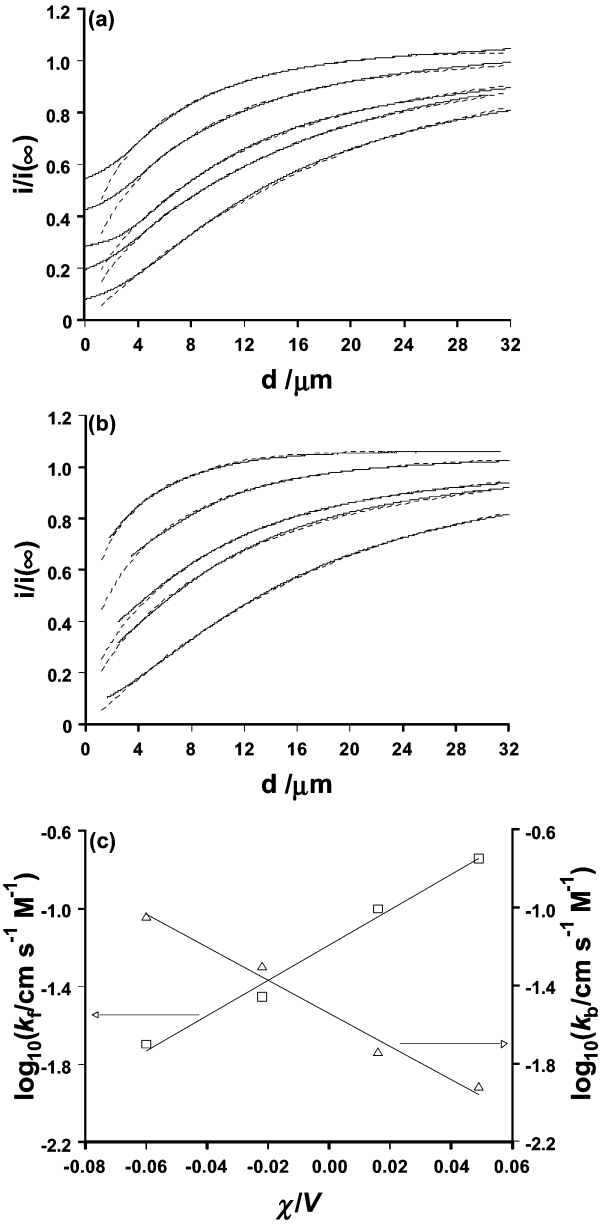

Fig. 5 Dependence of ET rate constants on driving force for the aqueous/NB system. (a) SECM approach curves (ferricyanide reduction) for the forward reaction with 10 mM TCNQ and 0.1 M THAP in the NB phase. From top to bottom, the first four solid experimental curves are for the following aqueous conditions: $[ClO_4^-]_w = 0.01$, 0.025, 0.1 and 0.25 M (1 mM $Fe(CN)_6^{3-}$ and 0.1 M NaCl) in the aqueous phase. The corresponding dashed theoretical curves, top to bottom, are for $k_f = 0.18$, 0.1, 0.035 and 0.02 cm s^{-1} M^{-1}. The lowest solid experimental curve was obtained in the absence of TCNQ in NB and the corresponding dashed curve is the theory for negative feedback. (b) SECM approach curves (TCNQ reduction) for the reverse reaction with 1 mM TCNQ and 0.1 M THAP in NB. From top to bottom, the first four solid experimental curves are for $[ClO_4^-]_w = 0.25$, 0.1, 0.025 and 0.01 M (20 mM $Fe(CN)_6^{3-}$ and 0.1 M NaCl) in the aqueous phase. The corresponding dashed theoretical curves, top to bottom, are for $k_b = 0.09$, 0.05, 0.018 and 0.012 cm s^{-1} M^{-1}. The lowest solid experimental curve was obtained in the absence of $Fe(CN)_6^{3-}$ in the aqueous phase and the corresponding dashed curve is the theory for negative feedback. (c) Tafel plot of data in (a, □) and (b, △), constructed using eqns. (7) and (8).

$Fe(CN)_6^{4-}$ is consumed simultaneously. This is most likely to be the transfer of $TCNQ^{\bullet -}$ from NB to the aqueous phase. $TCNQ^{\bullet -}$ could either react with $Fe(CN)_6^{3-}$, generating $Fe(CN)_6^{4-}$ or be directly detected by oxidation at the UME tip.

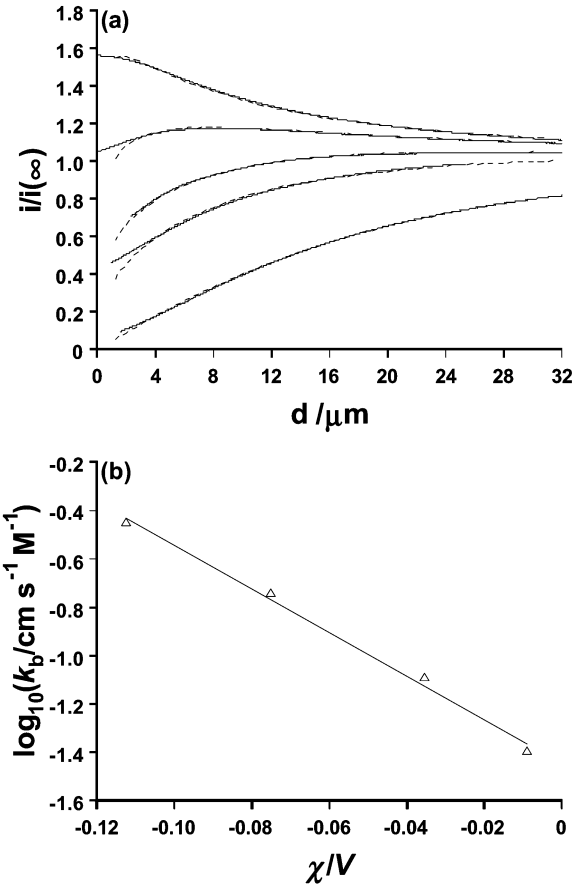

Fig. 6 Dependence of the reverse ET rate constants on driving force for the aqueous/NB system. (a) SECM approach curves (TCNQ reduction) obtained with 1 mM TCNQ and 0.01 M THAP in the NB phase. From top to bottom, the first four solid experimental curves are for $[ClO_4^-]_w = 0.25$, 0.1, 0.025 and 0.01 M (20 mM $Fe(CN)_6^{3-}$ and 0.1 M NaCl) in the aqueous phase. The corresponding dashed theoretical curves, top to bottom, are for $k_b = 0.3$, 0.18, 0.08 and 0.04 cm s^{-1} M^{-1}. The lowest solid experimental curve was obtained in the absence of $Fe(CN)_6^{3-}$ in the aqueous phase and the corresponding dashed curve is the theory for negative feedback. (b) Tafel plot (eqn. (8)) of data in a.

Analysis of ET rate constants using Marcus theory

We have observed that the rate constants depend strongly on interfacial potential drop, consistent with some previous SECM studies,[1–5] which suggested that Marcus theory[30] can be applied to ET at the ITIES. Since ET at the aqueous/NB interface may be complicated by the transfer of $TCNQ^{\bullet -}$, we focus on the results for ET in the aqueous/DCE system.

Marcus theory for ET at the ITIES considers the liquid/liquid interface as either a sharp boundary or a region which is several molecular layers thick.[30] Molecular dynamics simulations of the water/DCE system show a picture of the interface which is molecularly sharp on the shortest timescales, with finger-like distortions due to one solvent penetrating the other. These distortions extend up to 8 Å on a timescale of a few nanoseconds.[31,32] Over a longer timescale the result is a surface roughness of the same scale, with a change from the bulk of one phase to the other occurring over a distance of *ca.* 8–10 Å, as observed experimentally.[33,34]

The dependence of the ET rate constant on the driving force has a similar form for the two Marcus models.[30d] For the case where the interface is sharp and cannot be crossed by the reactants, the bimolecular electron transfer rate constant, k'_{12} (units m^4 s^{-1}) is given by:

$$k'_{12} = 2\pi(a_1 + a_2)\Delta\rho^3\kappa\nu\exp(-\Delta G^{\neq}/RT) \qquad (9)$$

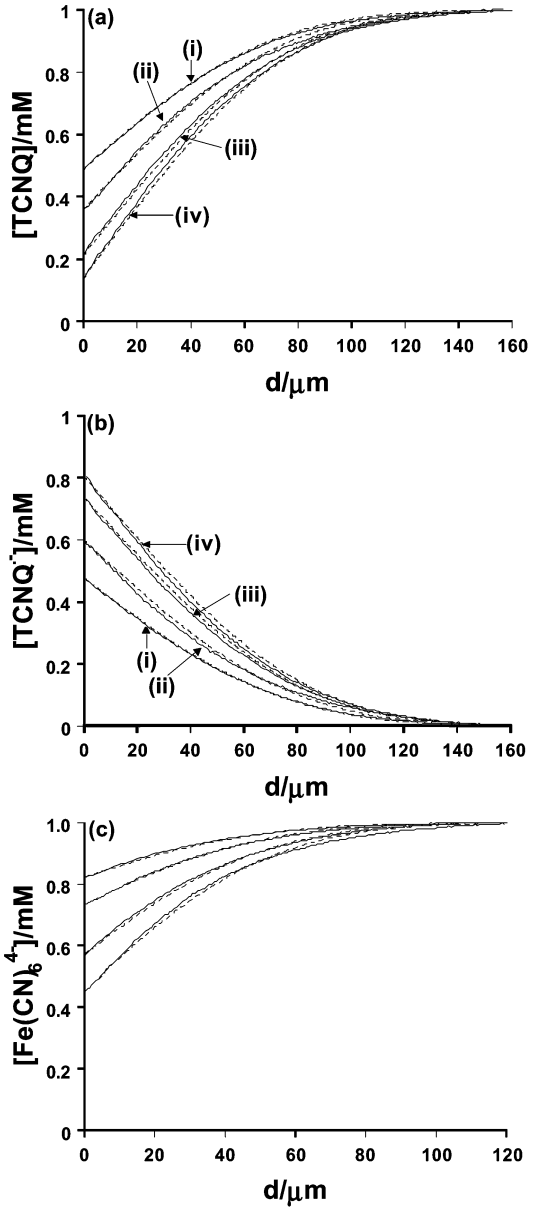

Fig. 7 MEMED concentration profiles (solid curves) for the aqueous/DCE system. (a) TCNQ concentration profiles obtained with 1 mM TCNQ and 0.01 M THAP in the DCE receptor phase, 50 mM $Fe(CN)_6^{4-}$, 0.1 M NaCl and (from top to bottom) 0.25 (i), 0.1 (ii), 0.025 (iii) and 0.01 M (iv) $NaClO_4$ in the aqueous droplet phase. Drop time and final drop radii were 6.3 s and 0.5 mm, respectively. Corresponding dashed theoretical curves, from top to bottom, are for $k_f = 0.03$, 0.05, 0.1 and 0.16 cm s^{-1} M^{-1}. (b) $TCNQ^{\bullet-}$ concentration profiles obtained with (from bottom to top) 0.25 (i), 0.1 (ii), 0.025 (iii) and 0.01 M (iv) $NaClO_4$ in the aqueous droplet phase and other parameters already cited in (a). Corresponding dashed theoretical curves, from bottom to top, are for $k_f = 0.03$, 0.05, 0.1 and 0.16 cm s^{-1} M^{-1}. (c) $Fe(CN)_6^{4-}$ concentration profiles obtained with 10 mM TCNQ and 0.01 M THAP in the DCE droplet phase, 1 mM $Fe(CN)_6^{4-}$, 0.1 M NaCl and (from top to bottom) 0.25, 0.1, 0.025 or 0.01 M $NaClO_4$ in the aqueous receptor phase and other parameters as for (a). Corresponding dashed theoretical curves, from top to bottom, are for $k_f = 0.03$, 0.05, 0.1 and 0.16 cm s^{-1} M^{-1}.

For an interface that is several molecular layers deep, of thickness, L, the expression for the corresponding rate constant, denoted by k''_{12} is:

$$k''_{12} = 4\pi(a_1 + a_2)^2 \Delta\rho\kappa\nu L \exp(-\Delta G^{\neq}/RT) \qquad (10)$$

In eqns. (9) and (10), a_1 and a_2 are the radii of the reactants, $\Delta\rho$ describes the distance dependence of the electron transfer

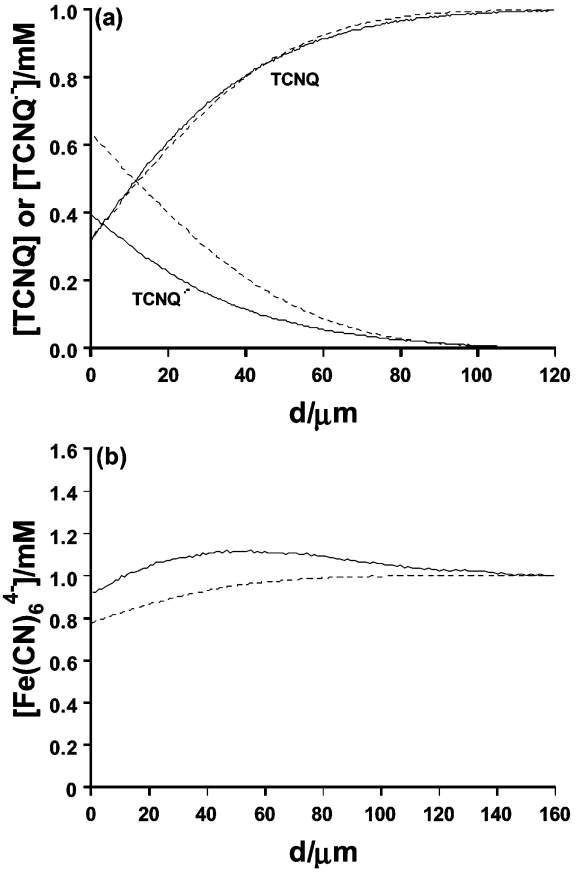

Fig. 8 MEMED concentration profiles (solid curves) for the aqueous/NB system. (a) 1 mM TCNQ and 0.01 M THAP in the NB receptor phase, with 50 mM $Fe(CN)_6^{4-}$, 0.1 M NaCl and 0.01 M $NaClO_4$ in the aqueous droplet phase. (b) 1 mM $Fe(CN)_6^{4-}$, 0.1 M NaCl and 0.01 M $NaClO_4$ in the aqueous receptor phase, with 10 mM TCNQ and 0.01 M THAP in the NB droplet phase. Drop time and final drop radii were 6.3 s and 0.5 mm, respectively. The dashed theoretical curves are concentration profiles for each species with $k_f = 0.04$ cm s^{-1} M^{-1}.

rate, usually denoted by β^{-1} in the literature,[35] with a typical value of 1 Å. The parameter κ is the Landau–Zener transmission coefficient and ν is a typical frequency of molecular motion. It is usual to consider $\kappa\nu \approx 10^{13}$ s^{-1}.

For the case of work term corrected rate constants,[30] $\Delta G^{\neq}$ for the sharp boundary model is given by:

$$\Delta G^{\neq} = (\lambda/4)(1 + \Delta G^{o\prime}/\lambda)^2 \qquad (11)$$

where $\Delta G^{o\prime} = -F\chi$, is the formal Gibbs energy for the one-electron transfer process and λ is the reorganisation energy.

It is convenient to define the equilibrium potential as the situation when the forward and reverse bimolecular rate constants are equal. This is seen to be close to $\chi = 0$ on the plots in Fig. 4(c) and 5(c), but does not correspond exactly because no account has been taken of the work terms on the driving force. While it is possible to estimate work terms in infinitely dilute solution, it is much more difficult for strong electrolyte solutions,[30] as employed in these studies. However, the work terms are relatively minor in infinitely dilute solution and will decrease further in electrolyte solution,[36] which serves to minimise electrostatic contributions and also decreases the effective charge density on highly charged moieties, such as ferro–ferricyanide, through ion pairing. We thus estimate that these terms will amount to only a few kJ mol^{-1} for this system, which is the order of the displacement from $\chi = 0$ of the potential where $k_f = k_b$.

In eqn. (11), the reorganisation energy is defined by $\lambda = \lambda_o + \lambda_i$, where λ_o and λ_i are the outer and inner sphere

reorganisation energies, respectively. λ_i is 39.7 kJ mol^{-1} for $Fe(CN)_6^{3-/4-}$ and 10 kJ mol^{-1} for the $TCNQ^{0/\bullet-}$ couple.[8] λ_i for bimolecular ET can be approximated using the mean value of λ_i of the two redox couples, while λ_o is given by,[30b]

$$\lambda_o = \frac{N_A(\Delta e)^2}{8\pi a_1 \varepsilon_o}\left(\frac{1}{D_1^{op}} - \frac{1}{D_1^{s}}\right) + \frac{N_A(\Delta e)^2}{8\pi a_2 \varepsilon_o}\left(\frac{1}{D_2^{op}} - \frac{1}{D_2^{s}}\right) - \frac{N_A(\Delta e)^2}{16\pi d_1 \varepsilon_o}\left(\frac{D_2^{op} - D_1^{op}}{D_1^{op}\left(D_2^{op} + D_1^{op}\right)} - \frac{D_2^{s} - D_1^{s}}{D_1^{s}\left(D_2^{s} + D_1^{s}\right)}\right) - \frac{N_A(\Delta e)^2}{16\pi d_2 \varepsilon_o}\left(\frac{D_1^{op} - D_2^{op}}{D_2^{op}\left(D_2^{op} + D_1^{op}\right)} - \frac{D_1^{s} - D_2^{s}}{D_2^{s}\left(D_2^{s} + D_1^{s}\right)}\right) - \frac{N_A(\Delta e)^2}{2\pi R_d \varepsilon_o}\left(\frac{1}{D_1^{op} + D_2^{op}} - \frac{1}{D_1^{s} + D_2^{s}}\right) \quad (12)$$

where D_1^{op} and D_2^{op} are the optical dielectric constants of the two phases (1.78 for water and 2.09 for DCE), ε_o is the permittivity of free space, D_1^{s} and D_2^{s} are the static dielectric constants of the two solvents (78.4 for water and 10 for DCE) and Δe is the charge transferred. The parameters d_1 and d_2 are the distances from the two reactants to the interface and we approximate these distances by the radii of the two reactants. $R_d \approx d_1 + d_2$ is the characteristic distance separating the two reactants and N_A is Avogadro's number. Considering $a_1 \approx a_2 \approx 4$ Å, the outer sphere reorganisation energy amounts to *ca.* 80 kJ mol^{-1}, so the overall reorganisation energy is 105 kJ mol^{-1}.

The bimolecular rate constant at the equilibrium potential based on the sharp boundary model is thus readily calculated as $k'_{12} = 0.08$ cm s^{-1} M^{-1} (converting units for comparison with experiment). Given the approximations involved in some of the parameters for the calculations, this result is in close agreement with the experimentally measured values of 0.08 cm s^{-1} M^{-1} (Fig. 4(c)) and 0.04 cm s^{-1} M^{-1} (Fig. 5(c)) when the forward and back bimolecular rate constants are equal. To apply the thicker layer model we shall assume that λ_o in the layer is given by eqn. (12). As pointed out by Marcus,[30d] there are various elaborations on this model that could be considered. With $L = 8$ Å, a much larger equilibrium bimolecular rate constant of $k''_{12} = 10$ cm s^{-1} M^{-1} results. For both calculations, work term contributions to $\Delta G^{\neq}$ have been neglected, but this is reasonable because this would amount to no more than a few percent compared to the reorganisation energy.

This comparison of the experimentally measured rate constants at zero standard free energy with theory indicates that the model in which the ITIES is sharp at the molecular level appears to be most appropriate. Consistency with this model is one of the reasons why Butler–Volmer kinetics are observed, particularly when the supporting electrolyte concentration in both phases is relatively high. On the other hand it is important to point out that more sophisticated analysis with the thicker layer model could yield results closer to those found experimentally.

Brief comment on the effect of aqueous ionic strength on the ET reaction

In our previous study,[4] we observed that the apparent ET rate constant decreased when the ionic strength in the aqueous phase increased by addition of an indifferent electrolyte and attributed this to a 'salting out effect'.[4] Similar experimental results were also obtained later by Bard and co-workers.[3] The latter study suggested that the effect of ionic strength on the ET kinetics could be due to several factors, *e.g.* double layer effects, specific or nonspecific adsorption, partitioning of the ions, coupled ET-ion transfer (IT), IT–IT coupling as well as salting-out effects. As the redox potential of $Fe(CN)_6^{3-/4-}$ is influenced by ionic strength in the aqueous phase,[5] we have re-analysed earlier data by carefully measuring the formal potential over the range of conditions of interest.[4]

The results of this analysis show that the α value is not significantly influenced by ionic strength in the aqueous phase within the range of interest ($\alpha = 0.43 \pm 0.04$ when $[THAP]_o = 0.1$ M and $\alpha = 0.34 \pm 0.02$ when $[THAP]_o = 0.01$ M). Rather, the apparent decrease in the rate constant observed with increasing ionic strength in the aqueous phase is due to a decrease in the driving force for the reaction from the effect of ionic strength on the formal potential for the ferro–ferricyanide couple, which was originally approximated as invariant with ionic strength. Similar effects are seen with Li_2SO_4 as the aqueous supporting electrolyte. In this case, $\alpha = 0.70 \pm 0.07$ (with $[THAP]_o = 0.10$ M and $[Li_2SO_4]_w = 0.10$ M), which is similar to $\alpha = 0.66 \pm 0.06$ (with $[THAP]_o = 0.1$ M and $[Li_2SO_4]_w = 0.50$ M) and $\alpha = 0.50 \pm 0.02$ (with $[THAP]_o = 0.01$ M and $[Li_2SO_4]_w = 0.50$ M). These results suggest that concentration effects[7,17,18] at the aqueous side of the interface are unimportant, consistent with the earlier work of Girault and co-workers.[7]

Summary and conclusions

Both SECM and MEMED have been used to investigate the effect of galvanic potential on the ET rate constant for the reaction between TCNQ and $Fe(CN)_6^{4-}$, and the reverse process. A wide range of conditions have been considered, covering two organic solvents and different organic electrolyte concentrations. ET coefficients close to 0.5 have been determined for all of the conditions explored.

Although SECM approach curves for ET in the aqueous/NB system fit well to theory, MEMED has highlighted that $TCNQ^{\bullet-}$ transfers from NB to the aqueous phase under the defined experimental conditions. This result illustrates the utility of MEMED as a sensitive probe of coupled IT processes during ET at the ITIES.

Experimental data for the aqueous/DCE system have been analysed further using Marcus theory. At equilibrium (when the forward and back ET rate constants are equal), the sharp boundary model for the ITIES predicts a bimolecular rate constant close to that measured experimentally. Consistency with this model is a reason why a Butler/Volmer kinetic formalism describes ET at the ITIES when the supporting electrolyte concentration in both phases is relatively high. Analysis of earlier experimental results,[4,5] has established that concentration effects[7,17] at the aqueous side of the ITIES are unimportant.

Acknowledgements

We thank the EPSRC for support of this work. JZ thanks the ORS scheme, the University of Warwick and Avecia for scholarships. Helpful discussions with Dr. John Atherton (Avecia, Huddersfield) are much appreciated.

References

1 (*a*) M. Tsionsky, A. J. Bard and M. V. Mirkin, *J. Phys. Chem. B*, 1996, **100**, 17 881; (*b*) M. Tsionsky, A. J. Bard and M. V. Mirkin, *J. Am. Chem. Soc.*, 1997, **119**, 10 785.
2 A. L. Barker, P. R. Unwin, S. Amemiya, J. Zhou and A. J. Bard, *J. Phys. Chem. B*, 1999, **103**, 7260.
3 Z. Ding, B. Quinn and A. J. Bard, *J. Phys. Chem. B*, 2001, **105**, 6367.
4 J. Zhang and P. R. Unwin, *J. Phys. Chem. B*, 2000, **104**, 2341.
5 A. L. Barker, P. R. Unwin and J. Zhang, *Electrochem. Commun.*, 2001, **3**, 372.
6 C. Shi and F. C. Anson, *J. Phys. Chem. B*, 2001, **105**, 8963.

7 Z. Ding, D. J. Fermin, P. F. Brevet and H. H. Girault, *J. Electroanal. Chem.*, 1998, **458**, 139.
8 Y. Cheng and D. J. Schiffrin, *J. Chem. Soc., Faraday Trans.*, 1993, **89**, 199.
9 Z. Samec, V. Marecek, J. Weber and D. Homolka, *J. Electroanal. Chem.*, 1981, **126**, 105.
10 D. J. Fermin, Z. Ding, D. H. Duong, P. F. Brevet and H. H. Girault, *J. Phys. Chem. B*, 1998, **102**, 10 334.
11 D. J. Fermin, D. H. Duong, Z. Ding, P. F. Brevet and H. H. Girault, *Phys. Chem. Chem. Phys.*, 1999, **1**, 1461.
12 D. J. Fermin, D. H. Duong, Z. Ding, P. F. Brevet and H. H. Girault, *J. Am. Chem. Soc.*, 1999, **121**, 10 203.
13 (*a*) C. Shi and F. C. Anson, *J. Phys. Chem. B*, 1998, **102**, 9850; (*b*) C. Shi and F. C. Anson, *J. Phys. Chem.*, 1999, **103**, 6283.
14 J. Zhang, A. L. Barker and P. R. Unwin, *J. Electroanal. Chem.*, 2000, **483**, 95.
15 A. L. Barker and P. R. Unwin, *J. Phys. Chem. B.*, 2000, **104**, 2330.
16 B. Liu and M. V. Mirkin, *J. Am. Chem. Soc.*, 1999, **121**, 8352.
17 W. Schmickler, *J. Electroanal. Chem.*, 1997, **429**, 123.
18 H. H. Girault, in *Modern Aspects of Electrochemistry*, ed. J.O'M. Bockris, B. E. Conway and R. E. White, Plenum Press, New York, 1993, vol. 25, p. 1.
19 (*a*) Y. Cheng and D. J. Schiffrin, *J. Chem. Soc., Faraday Trans.*, 1994, **90**, 2517; (*b*) R. A. W. Dryfe, R. D. Webster, B. A. Coles and R. G. Compton, *Chem. Commun.*, 1997, 779; (*c*) Z. Ding, P. F. Brevet and H. H. Girault, *Chem. Commun.*, 1997, 2059; (*d*) R. D. Webster, R. A. W. Dryfe, B. A. Coles and R. G. Compton, *Anal. Chem.*, 1998, **70**, 792.
20 J. V. Macpherson and P. R. Unwin, *J. Phys. Chem.*, 1994, **98**, 1704.
21 (*a*) C. J. Slevin, J. A. Umbers, J. H. Atherton and P. R. Unwin, *J. Chem. Soc., Faraday Trans.*, 1996, **92**, 5177; (*b*) C. J. Slevin, J. V. Macpherson and P. R. Unwin, *J. Phys. Chem. B*, 1997, **101**, 10 851; (*c*) A. L. Barker, J. V. Macpherson, C. J. Slevin and P. R. Unwin, *J. Phys. Chem. B*, 1998, **102**, 1586.
22 Y. Shao, M. V. Mirkin and J. F. Rusling, *J. Phys. Chem. B*, 1997, **101**, 3202.
23 J. Kwak and A. J. Bard, *Anal. Chem.*, 1989, **61**, 1221.
24 C. J. Slevin, P. R. Unwin and J. Zhang, in *Liquid Interfaces in Chemical, Biological, and Pharmaceutical Applications*, ed. A. G. Volkov, Marcel Dekker, New York, 2001, p. 325.
25 (*a*) C. J. Slevin and P. R. Unwin, *Langmuir*, 1997, **13**, 4799; (*b*) C. J. Slevin and P. R. Unwin, *Langmuir*, 1999, **15**, 7361; (*c*) J. Zhang, C. J. Slevin and P. R. Unwin, *Chem. Commun.*, 1999, 1501; (*d*) J. Zhang and P. R. Unwin, *Phys. Chem. Chem. Phys.*, 2000, **2**, 1267; (*e*) J. Zhang, C. J. Slevin, L. Murtomäki, K. Kontturi, D. E. Williams and P. R. Unwin, *Langmuir*, 2001, **17**, 821.
26 N. Eugster, D. J. Fermin and H. H. Girault, *J. Phys. Chem. B*, 2002, **106**, 2428.
27 J. Zhang, PhD thesis, University of Warwick, 2001.
28 A. J. Bard and L. R. Faulkner, *Electrochemical Methods*, Wiley, New York, 1980.
29 C. Beriet and D. Pletcher, *J. Electroanal. Chem.*, 1993, **361**, 93.
30 (*a*) R. A. Marcus, *J. Phys. Chem.*, 1990, **94**, 1050; (*b*) R. A. Marcus, *J. Phys. Chem.*, 1990, **94**, 4152; (*c*) R. A. Marcus, *J. Phys. Chem.*, 1990, **94**, 7742; (*d*) R. A. Marcus, *J. Phys. Chem.*, 1991, **95**, 2010; (*e*) R. A. Marcus, *J. Phys. Chem.*, 1995, **99**, 5742.
31 I. Benjamin, *J. Chem. Phys.*, 1992, **97**, 1432.
32 I. Benjamin, *Chem. Rev.*, 1996, **96**, 1449.
33 J. Strutwolf, A. L. Barker, M. Gonsalves, D. J. Caruana, P. R. Unwin, D. E. Williams and J. R. P. Webster, *J. Electroanal. Chem.*, 2000, **483**, 163.
34 C. Wei, A. J. Bard and M. V. Mirkin, *J. Phys. Chem.*, 1995, **99**, 16 033.
35 R. A. Marcus and N. Sutin, *Biochim. Biophys. Acta*, 1985, **811**, 265.
36 L. Eberson, *Electron Transfer Reactions in Organic Chemistry*, Springer-Verlag, Berlin, 1987, p. 27.